Submitted to EPSL, 16/05/06

Review comments received 26/05/06

Submitted in revised form 08/06/06

"Explosive Energy" During Volcanic Eruptions from Fractal Analysis of Pyroclasts

Ulrich Kueppers[1*], Diego Perugini[2], Donald B. Dingwell[1]

[1] Earth & Environmental Sciences, Ludwig-Maximilians-Universität München (LMU),

Theresienstrasse 41, 80333 München, Germany

[2]Department of Earth Sciences, University of Perugia, Piazza Università 1, 06100, Perugia, Italy

[*]Corresponding author:

E-mail: ulli@min.uni-muenchen.de

Tel: +49 89 21804221

Fax: +49 89 21804176

Abstract

Despite recent advances by means of experiments and high-resolution surveys and the growing understanding of the physical processes before and during volcanic eruptions, duration and type of eruptive activity still remain highly unpredictable. This uncertainty hinders appropriate hazard and associated risk assessment tremendously. In an effort to counter this problem, experimentally generated pyroclasts have been studied by fractal statistics with the aim of evaluating possible relationships between eruption energy and fragmentation efficiency.

Rapid decompression experiments have been performed on three differently porous sample sets of the 1990-1995 eruption of Unzen volcano (Japan) at 850 °C and at initial pressure values above the respective fragmentation threshold [1, 2]. The size distribution of generated pyroclasts has been studied by fractal fragmentation theory and the fractal dimension of fragmentation (D_f), a value quantifying the intensity of fragmentation, has been measured for each sample. Results show that size distribution of pyroclastic fragments follows a fractal law (i.e. power-law) in the investigated range of fragment sizes, indicating that fragmentation of experimental samples reflects a scale-invariant mechanism. In addition, D_f is correlated positively with the potential energy for fragmentation (PEF) while showing a strong influence of the open porosity of the samples.

Results obtained in this work indicate that fractal fragmentation theory may allow for quantifying fragmentation processes during explosive volcanic eruptions by calculating the fractal dimension of the size distribution of pyroclasts. It emerges from this study that fractal dimension may be utilised as a proxy for estimating the explosivity of volcanic eruptions by analysing their natural pyroclastic deposits.

Keywords

Volcanic fragmentation, simulation of eruptions, explosive energy, pyroclasts, fragment size distribution, fractal fragmentation theory.

1. Introduction

In the past few decades, many factors influencing brittle fragmentation of magma have been recognised and their contribution to volcanic eruptions elucidated [e.g. 3-5]. The fragmentation bomb as introduced by Alidibirov and Dingwell [6] and developed by Spieler et al. [2] has been proven to be a suitable device to simulate decompression-driven volcanic eruptions in the laboratory. The use of natural samples has enabled the investigation of a wide variety of physical parameters acting during magma fragmentation.

Although the improvement in simulating explosive eruptions has resulted in a better understanding of the associated physical processes, a systematic statistical analysis of fragments generated by experiments is still incomplete. Such an approach however may give new insights into the interplay between eruption energy, applied pressure, and the style of fragmentation.

Several studies [e.g. 7-9] have shown that the fragmentation process can be approximated by a hierarchical mechanism propagating from large scales to small scales associated to the development of a fractal network of cracks. In particular, the application of fractal fragmentation theory has been demonstrated to be useful in unravelling unexpected correlations between the fragmentation process and the fractal dimension of size distribution generated in a variety of contexts from soil cracking to rock fracturing under various experimental and natural conditions [e.g. 8, 10-14].

In our continuing efforts to compare and combine results from laboratory experiments in the fragmentation bomb and thorough analysis of natural deposits, the grain-size distributions of experimentally generated pyroclasts are investigated here for their fractal distribution. In particular, the fractal fragmentation theory is applied to fragment size distributions obtained under different pressurizations for samples with different open porosity, and the fractal dimension

of such distributions is measured. The results are discussed in the light of their possible applicability in the study of natural pyroclastic deposits to estimate the eruptive energy of past eruptions.

2. Fragmentation experiments and sampling

The samples employed here derive from block-and-ash flow deposits of the 1990-1995 Unzen eruption and were collected in 2001. Three sets of samples representing values of open porosity of 7.0 vol.% (MUZ A), 20.5 vol.% (MUZ C), and 35.5 vol.% (MUZ F) have been chosen. A more detailed sample description can be found in Kueppers et al. [1].

Fragmentation experiments were performed in the fragmentation bomb [6], modified as described by Spieler et al. [2] (Figure 1). It is a shock tube type apparatus that permits simulation of volcanic conditions in terms of temperature, gas overpressure, and rate of decompression. The experimental set-up consists of three units [15]:

- A low-pressure tank (inner dimensions: diameter = 40 cm, length = 300 cm) at ambient pressure where the experimentally generated pyroclasts collect.
- A pressurization system with up to three diaphragms, each of which opens at a certain pressure differential.
- A high-pressure, high-temperature steel autoclave (length = 45 cm) separated from the low-pressure tank by the diaphragms.

All experiments were heated externally to 850 °C and pressurised with Argon. Initial overpressure conditions above the sample's threshold [2] lead to complete sample fragmentation. The pyroclasts generated have been flushed from the low-pressure tank with distilled water through a 250 µm sieve and thereby separated into a coarse and a fine fraction. As the experimental set-up is gastight, the sample yield is very high (loss < 0.4 wt.%). Dry sieving was

performed at half-Φ steps (Φ =-$Log_2(d)$, with d = particle diameter in millimetre; e.g. [16] or literature cited therein). In this study, only the coarse fraction (i.e. > 250 μm) has been used. It is important to note that the experimentally generated pyroclast sample does not reflect any transport-related sorting.

The potential energy for fragmentation (PEF) is defined as the expansive force of the compressed gas. It is different in each experiment as it depends on the sample size (V_{cyl} [m^3]), the gas fraction (θ [dimensionless]) that corresponds to the open porosity of the respective sample, and the applied pressure (ΔP [Pa]). It was calculated as follows:

$$PEF\left[Joule\right] = V_{cyl} \cdot \theta \cdot \Delta P \qquad \text{Eq. 1}$$

During this study, the open porosity ranged from 7 to 35.5 wt.% and the applied pressure was as high as 50 MPa, resulting in PEF ranging from ca. 50 to 280 J.

3. Fractal analysis of experimentally generated pyroclasts: basic principles

As reported by Mandelbrot [7], Korcak [17] performed empirical studies on the size distribution of the areas of islands and developed the empirical relationship:

$$N(A > a) \approx a^{-b} \qquad \text{(Eq. 2)}$$

where $N(A>a)$ is the total number of islands having size A greater than a given comparative size, a, and b is a constant equal to 1/2 $(b=1/2)$ for all islands [9]. Mandelbrot [7] studied Korcak's [17] work and found that b actually varied between island regions with b always being greater than 1/2 $(b>1/2)$. In the light of fractal theory, he further realized that the size distribution of a population of islands was actually a consequence of fractal fragmentation and that the empirical constant 'b' correlated with the fragmentation fractal dimension. He therefore suggested that

fractal fragmentation could be quantified by measuring the fractal dimension through the equation

$$N(M > m) = km^{-D_f} \qquad \text{(Eq. 3)}$$

where D_f is the fragmentation fractal dimension, $N(M > m)$ is the total number of particles with linear dimension M which is greater than a given comparative size, m, and k is a proportionality constant. It is to note that D_f derived from Eq. (3) is not a measure of irregularity but a measure of the size-number relationship of the particle population or, in other terms, the fragmentation of the population. Taking the logarithm of both sides of Eq. (3) yields a linear relationship between $N(M > m)$ and m, where D_f is the slope coefficient.

Many size distributions in nature follow Korcak's [17] empirical law, including the fragmentation of rock into increasingly small pieces [e.g. 8] along zones of weakness (i.e. cracks). Independently of scale, cracks show repetitive branching leading to a tree of cracks (Brown and Wohletz [18]). One can therefore assume that the grain size distribution of particles generated by volcanic eruptions in general and the above described experiments in particular is fractal and that fractal dimensioning can thereby be used to quantify the size distribution.

In order to apply the number-based size relationship Eq. (3) to the analysis of fragments generated by simulated eruptions, assumptions must be made regarding the unit weight of individual particles, since particle size distribution is determined by mass comparison, i.e. mass retained on successive sieve sizes. The number-based size relationship can be used by modelling individual particles as uniform shapes, thereby developing uniform standard densities. By adjusting the size of the uniform particle to coincide with sieve screen dimensions, the number of particles bounded by each sieve can be determined by dividing the total weight of material retained on each sieve by the density of an individual particle.

4. Results

All results presented in this section refer to the size distribution of experimentally generated pyroclasts, not to surface textures. Although natural volcanic samples have been used, we assume that grain size and pyroclast density are independent. Figures 2A, C, and E show the variation of $N(M>m)$ against m for three representative samples with different open porosities, different values of applied pressure and thus different values of PEF. The graphs clearly display a power-law behaviour that can be even better seen in the Log[$N(M>m)$] vs. Log(m) graphs presented in Figures 2B, D, and F. Here, data points plot along straight lines defining very good linear trends (r~0.99 for all cases). These linear trends extend over approximately two orders of magnitude testifying to the fractal nature of the fragmentation process as predicted by the fractal fragmentation theory. D_f was estimated for all studied samples from the slope of the linear fitting of Log[$N(M>m)$] vs. Log(m). For the adjacent values, please refer to Table 1. Results show that D_f varies between 2.095 and 2.257, 2.271 and 2.497, and 2.370 and 2.553, for samples with 7%, 20.5%, and 35.5% open porosity, respectively. The systematic increase of D_f with PEF (Figures 3A-C) proves an increasing fragmentation efficiency (Wohletz and Brown [19], "maturity of the fragmentation process"). The graphs show that the increase of D_f is linear (r value of linear fitting > 0.95) with most samples laying inside 95% of confidence of the fitting (dashed lines). Figure 3D is a comprehensive plot of Figures 3A-C and highlights that the rate of increase of D_f with PEF is depending on the open porosity, indicated by the fact that the slope of linear fitting of data decreases as open porosity increases. In Figures 4A and B, the variation of the intercept and slope of linear fitting of data presented in Figure 3 is plotted against the open porosity of samples. It becomes obvious that the intercept of linear fitting is positively, the slope of linear fitting negatively correlated with the open porosity. We would like to point out that the variation of intercept and the slope of linear fitting are significant for the three sets of samples, i.e. well

outside errors estimated with linear regression. On the basis of these results it is possible to derive three linear equations relating D_f and PEF for the three values of studied open porosities:

7% open porosity → $D_f = 2.60^{-3} PEF + 1.97$ (Eq. 4)

20.5% open porosity → $D_f = 1.78^{-3} PEF + 2.15$ (Eq. 5)

35.5% open porosity → $D_f = 8.96^{-4} PEF + 2.31$ (Eq. 6)

The results can be summarized as follows:

1) The fragment size distribution of experimentally generated pyroclasts is consistent with fractal fragmentation theory in that size distributions are fractals and they can be univocally quantified by measuring a single parameter, i.e. D_f.

2) There is a well constrained linear increase of D_f with PEF for all three sets of samples.

3) The degree of increase of D_f with PEF is depending on the open porosity of the investigated samples. In particular, the higher the open porosity, the lower the increase of D_f with PEF.

5. Implications

The above described findings derive from hot rapid decompression experiments on natural volcanic samples. In terms of the acting physical processes, these experiments are comparable to magmatic, volcanic eruptions. We evaluated the size distribution of experimental pyroclasts as a function of porosity and applied pressure and showed that the achieved fragment size distributions may be studied by fractal fragmentation theory.

As the fragmentation efficiency (i.e. D_f) shows a linear dependency of open porosity and the available energy that can be converted into fragmentation (i.e. PEF) (Figures 3 A-D), we propose that it is possible to estimate PEF by measuring values of D_f. The latter can be quantified by evaluating grain size distribution and open porosity. Considering that the variation of intercept

and slope display a linear, predictable variation with open porosity (Fig. 4A and B), analogous equations may be interpolated in the range of studied open porosities (7%-35.5%). This indicates that it is possible to derive a set of linear equations relating D_f and PEF and thereby proves again that PEF can be estimated by measuring D_f and open porosity of samples. As Figure 3 D (D_f vs. PEF) shows, the slope is decreasing as open porosity increases. This finding is not well understood yet, we assume that it might be related to bubble textures and the adjacent degassing behaviour.

There are some publications investigating the fragmentation and/or fractal behaviour of volcanic rocks. However, these studies had different approaches and investigated the fragmentation of basaltic melt [20], particle size-density relationships [21], the shapes of volcanic particles [22] or magmatic enclaves [23], fragmentation phenomena in magmatic crystals [24], or fragmentation behaviour of starting material at constant density [18]. To the best of our knowledge, this is the first investigation of pyroclast size with fractal theory. Our results from experimentally generated pyroclasts show that one can use the fractal theory to shed light into the mechanisms acting during volcanic fragmentation processes. A combination of thorough field and laboratory analysis and the investigation of the D_f of these volcanic deposits may represent a further tool towards a better understanding of the mechanisms acting during volcanic fragmentation. This aspect is particularly important because it constitutes the basis for developing a new approach in the study of natural volcanic deposits and, ultimately, may furnish new tools for volcanic eruption forecasting. In this respect, results presented in this paper may help in evaluating volcanic risk by estimating the explosivity (e.g. pressure in the conduit) during an eruptive event from the value of fractal dimension of fragment size distribution of the adjacent deposits. This may give the opportunity to draw iso-D_f or iso-explosivity maps that can be potentially helpful for hazard assessment and risk mitigation authorities.

The presented findings need to be tested on natural volcanic deposits to evaluate the influence and consequences of transport and sorting processes on the fractal dimension.

Acknowledgments

UK was financially supported by the Deutsche Forschungsgemeinschaft. DP was founded by MIUR (Ministero dell'Istruzione, dell'Università e della Ricerca) and Università degli Studi di Perugia grants. We would like to thank the two anonymous reviewers for their helpful comments and Betty Scheu for skype-discussions to Japan.

References

[1] U. Kueppers, B. Scheu, O. Spieler, D.B. Dingwell, Fragmentation efficiency of explosive volcanic eruptions: A study of experimentally generated pyroclasts. J. Volcanol. Geotherm. Res. 153 (2006) 125-135.

[2] O. Spieler, B. Kennedy, U. Kueppers, D.B. Dingwell, B. Scheu, J. Taddeucci, The fragmentation threshold of pyroclastic rocks. EPSL 226 (2004) 139-148.

[3] A.R. McBirney, T. Murase, Factors governing the formation of pyroclastic rocks. Bull. Volcanol. 34 (1970) 372– 384.

[4] D.B. Dingwell, Volcanic dilemma: flow or blow? Science 273 (1996) 1054– 1055.

[5] M. Alidibirov, D.B. Dingwell, Three fragmentation mechanisms for highly viscous magma under rapid decompression. J. Volcanol. Geotherm. Res. 100 (2000) 413–421.

[6] M. Alidibirov, D.B. Dingwell, An experimental facility for investigation of magma fragmentation by rapid decompression. Bull. Volcanol. 58 (1996) 411– 416.

[7] B.B. Mandelbrot, The fractal geometry of Nature. W.H. Freeman and Company, New York (1982).

[8] D.L. Turcotte, Fractals and chaos in geology and geophysics. Cambridge University Press (1992).

[9] G. Korvin, Fractal Models in the Earth Sciences. Elsevier, Amsterdam (1992).

[10] C.G. Sammis, R.H. Osborne, J.L. Anderson, M. Banerdt, P. White, Self-similar cataclasis in the formation of fault gouge. Pure and Applied Geophysics, 124 (1986) 191-213.

[11] M.K. Hassan, G.J. Rodgers, Models of fragmentation and stochastic fractals. Phys. Lett., A 208 (1995) 95– 98.

[12] E. Perfect, Fractal models for the fragmentation of rocks and soils: A review. Engin.

Geology, 48 (1997) 185-198.

[13] H. Millan, M. Gonzalez-Posada, R.M. Benito, Fragmentation fractal dimensions of Vertisol samples: influence of sieving time and soil pre-treatment. Geoderma, 109 (2002) 75-83.

[14] W. Barnett, Subsidence breccias in kimberlite pipes—an application of fractal analysis. Lithos, 76 (2004) 299-316.

[15] U. Kueppers, Nature and efficiency of pyroclast generation from porous magma: Insights from field investigations and laboratory experiments. PhD dissertation, University (LMU) of Munich (2005), http://edoc.ub.uni-muenchen.de/archive/00004587/

[16] R.A.F. Cas, J.V. Wright, Volcanic successions: modern and ancient. Chapman & Hall, London (1987) 476-478.

[17] J. Korcak, Deux types fondamentaux de distribution statistique. Bull. De l'Institute International de Statistique. 3 (1938) 295-299.

[18] W.K. Brown, K.H. Wohletz, Derivation of the Weibull distribution based on physical principles and its connection to the Rosin-Rammler and lognormal distributions. Journ. Of Appl. Phys. 78 (1995) 2758-2763.

[19] K.H. Wohletz, W.K. Brown, Particulate size distributions and sequential fragmentation/transport theory. Los Alamos National Laboratory report (1995) LA-UR 95-0371

[20] B. Zimanowski, R. Büttner, V. Lorenz, H.G. Häfele, Fragmentation of basaltic melt in the course of explosive volcanism. Journ. Geophys. Res. 102, B1 (1997) 803-814.

[21] J. Taddeucci, D.M. Palladino, Particle size-density relationships in pyroclastic deposits: inference for emplacement processes. Bull. Volcanol. 64 (2002) 273-284.

[22] A. Maria, S. Carey, Using fractal analysis to quantitatively characterize the shapes of volcanic particles. Journ. Geophys. Res. 107, B11 (2002) doi:10.1029/2001JB000822.

[23] D. Perugini, G. Poli, N. Prosperini, Morphometric analysis of magmatic enclaves: a tool for understanding magma vesiculation and ascent. Lithos 61 (2002) 225-235.

[24] I.N. Bindemann, Fragmentation phenomena in populations of magmatic crystals. Am. Mineral. 90 (2005) 1801-1815.

Figure captions

Figure 1: Schematic drawing and picture of the experimental set-up, the fragmentation bomb. The large tank is at ambient pressure and collects the pyroclasts. A set of three diaphragms maintains the pressure differential to the externally heated, high pressure autoclave, where the cylindrical sample is placed (after [2]).

Figure 2: (A-C-E) variation of $N(M>m)$ against m for three representative samples with different open porosities and different values of potential energy for fragmentation; (B-D-F) Log[$N(M>m)$] vs. Log(m) graphs showing the fractal nature of fragment size distribution generated by simulated volcanic eruptions; m values are given in millimetres.

Figure3: (A-C) Linear increase of fractal dimension of fragmentation (D_f) as the potential energy for fragmentation (PEF) increases for samples with different open porosity. Data points lay inside 95% of confidence of the fitting (dashes lines) as reported in the graphs; D) comparison, in a single plot, of data shown in A-C.

Figure 4: Variation of the intercept (A) and slope (B) of linear fitting of data presented in Figure 3 plotted against the open porosity of samples.

Table captions

Table 1: Results from fractal analysis of experimentally generated pyroclasts. In the table are reported values of applied pressure [ΔP (MPa)], potential energy for fragmentation [PEF], and fractal dimension of fragmentation [D_f] for three sets of samples with open porosites of 7% (A), 20.4% (B) and 35.5% (C).

Figure 1:

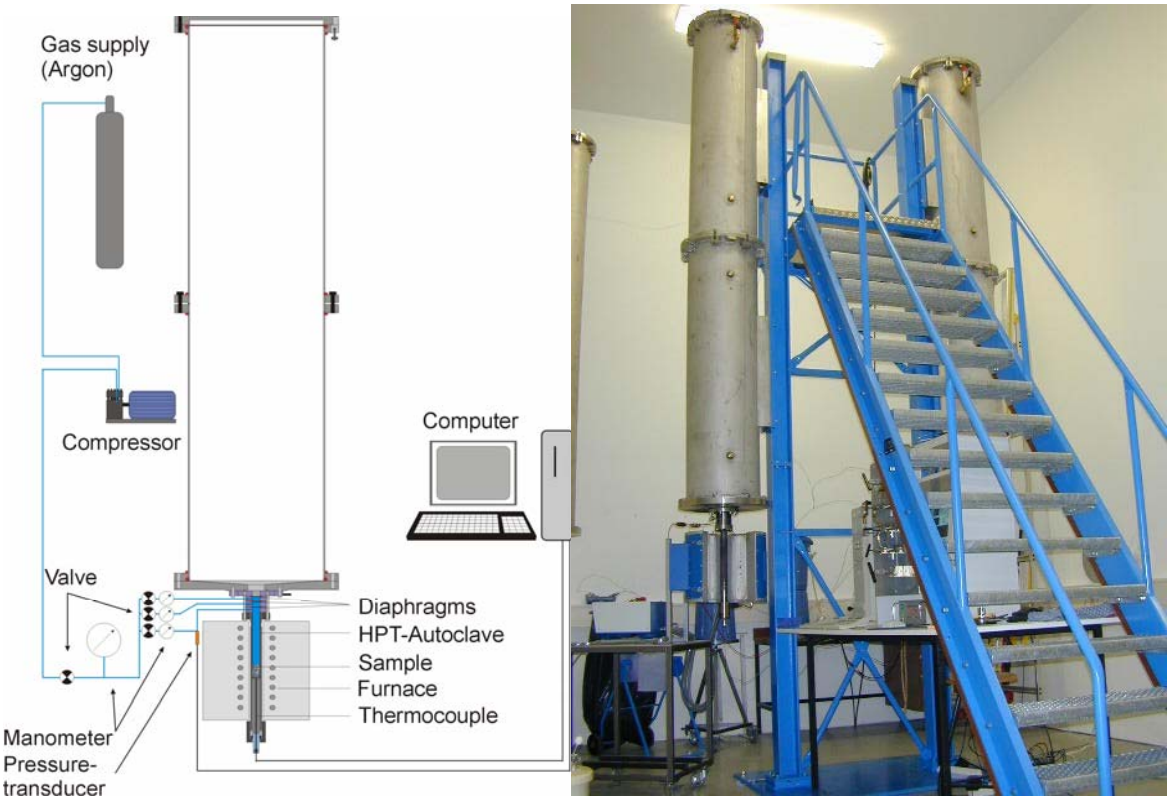
Gas supply
(Argon)
Compressor
Computer
Valve
Diaphragms
HPT-Autoclave
Sample
Furnace
Thermocouple
Manometer
Pressure-
transducer

Figure 2:

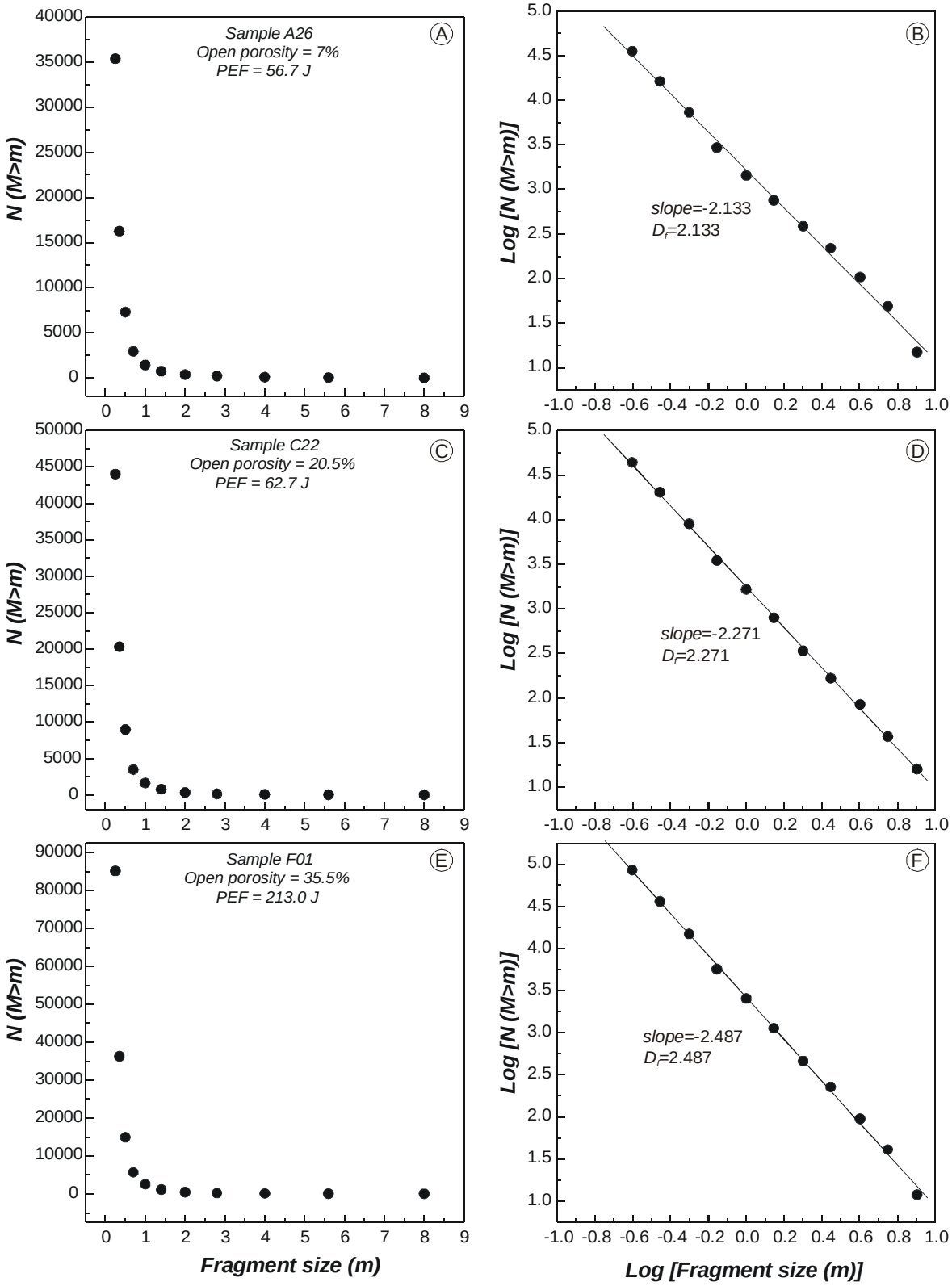
Sample A26
Open porosity = 7%
PEF = 56.7 J
Ⓐ
N (M>m)
Ⓑ
Log [N (M>m)]
slope=-2.133
D_f=2.133
Sample C22
Open porosity = 20.5%
PEF = 62.7 J
Ⓒ
Ⓓ
slope=-2.271
D_f=2.271
Sample F01
Open porosity = 35.5%
PEF = 213.0 J
Ⓔ
Ⓕ
slope=-2.487
D_f=2.487
Fragment size (m)
Log [Fragment size (m)]

Figure 3:

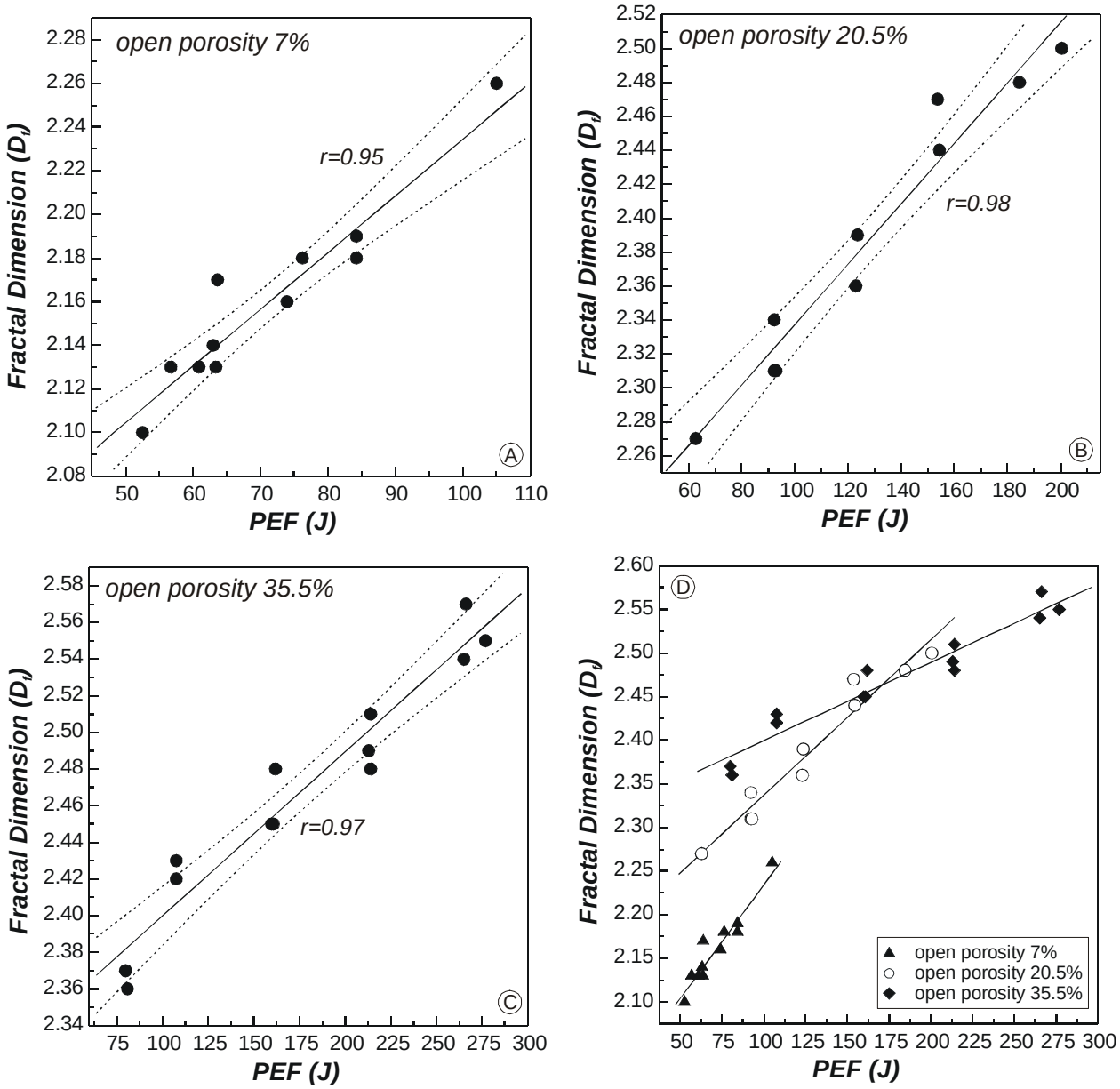
open porosity 7%
r=0.95
A
Fractal Dimension (D_f)
PEF (J)
open porosity 20.5%
r=0.98
B
open porosity 35.5%
r=0.97
C
D
open porosity 7%
open porosity 20.5%
open porosity 35.5%

Figure 4:

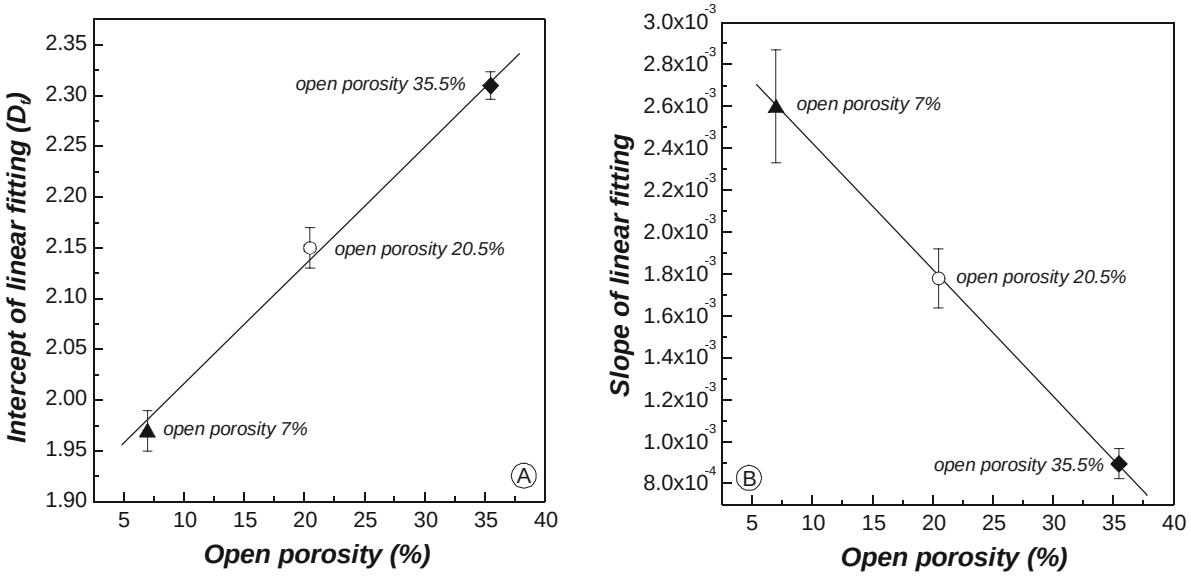
Intercept of linear fitting (D_f)
Open porosity (%)
open porosity 35.5%
open porosity 20.5%
open porosity 7%
A
Slope of linear fitting
Open porosity (%)
open porosity 7%
open porosity 20.5%
open porosity 35.5%
B

Table 1:

[A]

7% open porosity			
Sample	**ΔP (MPa)**	**Energy**	**D_f**
A 01	25,0	52,5	2,095
A 26	27,0	56,7	2,133
A 10	29,0	60,9	2,132
A 33	30,0	63,0	2,140
A 21	30,2	63,4	2,125
A 19	30,3	63,6	2,173
A 28	35,2	73,9	2,157
A 24	36,3	76,2	2,180
A 29	40,1	84,2	2,181
A 30	40,1	84,2	2,176
A 32	40,1	84,2	2,191
A 31	50,0	105,0	2,257

[B]

20.5% open porosity			
Sample	**ΔP (MPa)**	**Energy**	**D_f**
C 22	10,2	62,7	2,271
C 44	15,0	92,3	2,338
C 32	15,0	92,3	2,314
C 46	15,1	92,9	2,306
C 41	20,0	123,0	2,363
C 38	20,1	123,6	2,393
C 42	25,0	153,8	2,473
C 43	25,1	154,4	2,437
C 45	30,0	184,5	2,480
C 34	32,6	200,5	2,497

[C]

35.5% open porosity			
Sample	**ΔP (MPa)**	**Energy**	**D_f**
F 10	7,5	79,9	2,370
F 08	7,6	80,9	2,364
F 13	10,1	107,6	2,416
F 16	10,1	107,6	2,431
F 20	15,0	159,8	2,452
F 18	15,1	160,8	2,451
F 19	15,2	161,9	2,476
F 01	20,0	213,0	2,487
F 02	20,1	214,1	2,513
F 05	20,1	214,1	2,475
F 07	24,9	265,2	2,541
F 06	25,0	266,3	2,572
F 09	26,0	276,9	2,553